ISSN 2379-4038

LIVER RESEARCH
Open Journal

Openventio PUBLISHERS

Original Research

Correlation of ^{18F}-Fluorodeoxyglucose Glucose Uptake by Liver Cancer and Transcriptional Regulation of the Warburg Effects in ATT-MYC Mouse Model of Liver Cancer

Mahmoud Elalfy, PhD[1*]; Juergen Borlak, MD[2]

[1]*Forensic Medicine and Toxicology Department, Faculty of Veterinary Medicine, Mansoura University, Mansoura 35516, Egypt*
[2]*Centre for Pharmacology and Toxicology, Hannover Medical School, Carl-Neuberg-Str. 1, 30625, Hannover, Germany*

[*]***Corresponding author***
Mahmoud Elalfy, PhD
Associate professor, Forensic Medicine and Toxicology Department, Faculty of Veterinary Medicine, Mansoura University, Mansoura 35516, Egypt;
E-mail: mahmoudelalfy@mans.edu.eg

Article information
Received: January 17th, 2020; **Revised:** April 15rd, 2020; **Accepted:** May 5th, 2020; **Published:** May 16th, 2020

Cite this article
Elalfy M, Borlak J. Correlation of ^{18F}-fluorodeoxyglucose glucose uptake by liver cancer and transcriptional regulation of the warburg effects in ATT-MYC mouse model of liver cancer. *Liver Res Open J*. 2020; 3(1): 1-8. doi: 10.17140/LROJ-3-112

ABSTRACT

Background
It was previously reported that diethylnitrosamine (DEN) enhanced liver cancer progression in ATT-MYC mouse model of liver cancer. Radiogenomics is a new tool in advanced science technology that gives information on tumor biology, non-tumor surrounding tissue, the degree of tumor size and presence of necrosis of cells especially with joined micro computed tomography – positron emission tomographys (CT/PETs).

Aim
To evaluate the correlation of gene expression and non-invasive microPET information of the liver tumors at different points of the stage of growth.

Methods
Exon array expression of the liver of ATT-MYC mice treated with DEN or butylated hydroxytoluene (BHT) compared to control non-transgenic mice were analyzed by array track and the current data were also compared to microarray expression of liver tumor of ATT-MYC mice.

Results
The expression of genes responsible for glucose transport such as *glut1, 3, 4*, *hk1*, *slc1a5*, *slc1a1*, *slc1a4*, *slc1a2, gp6c* and *gpc-1-3-4* were up-regulated significantly in DEN-treated transgenic mice immediately after end of treatment ($p \leq 0.05$), while *glut2* (fold change 0.9503, *p*-value 0.4385) and *hk2* (fold change 3.0589, *p*-value 0.0565) genes were increased not significantly immediately after end of treatment. Additionally, at 4.5-months of observation after the end of treatment *slc1a5*, *slc38a2*, *glut1*, *glut4* and *gpc3-4* genes had a significant fold change in liver tumor tissue in DEN treated mice when compared to BHT or control transgenic or non-transgenic one. While *hk1, 2*, *slc5a1*, *slc1a4*, *glut2*, *glut3*, *g6pc* and *gpc-1* genes were increased non-significantly in the liver of treated mice when compared to control group at 4.5-months of observation after the end of treatment. Notably, *c-myc*, *hif-1* and *aldoa* glycolytic genes were expressed significantly both time points of 4 and 8.5-months while *ldhb*, *hk-2* and *PKM2* were increased non-significantly in DEN treatment when compared to BHT/control non-transgenic animals.

Conclusion
There is a definitive correlation between genes responsible for glucose transport and ^{18F}-Fluorodeoxyglucose (FDG) uptake in the early and advanced degree of liver carcinogenesis. This study of glucose pathway in Hepatocellular carcinoma (HCC) at different stages of early and advanced one is the potential for therapeutic anticancer therapy.

Keywords
$^{18-F}$Fluorodeoxyglucose (FDG); MicroPET; Exon array expression; Hepatocellular carcinoma (HCC); Att-myc transgenic mice; Diethylnitrosamine (DEN), Butylated hydroxytoluene (BHT); Glucose metabolism.

INTRODUCTION

Hepatocellular carcinoma (HCC) is a leading cause of cancer death in the United States[1] and considered the second leading cause of cancer death in East Asia and sub-Saharan Africa and the sixth most common in western countries.[2-4] The HCC occurred after chronic affection with hepatitis C, B, liver cirrhosis, Aflatoxin B1 exposure, hemochromatosis, fatty liver disease, alpha-1 antitrypsin deficiency, pesticides and chemical exposure.[4,5] The survival rate of HCC harboring patients is still low after using different protocols of treatment in the presence or absence of cirrhosis to the percentage of liver tumor tissue to non-tumor tissue based on therapy by positron emission tomography/computed tomography (PET/CT) imaging modalities.[6]

The correlation of ^{18F}-Fluorodeoxyglucose (FDG) glucose uptake and large volume of liver with tumor tissue in *c-myc* transgenic mice treated with diethyl-nitrosamine was reported by micro CT/PET imaging.[7] Genomics, radiogenomics or imaging, has new advanced tools in correlation science of different imaging modality data with genomic data. Radiogenomics science revealed detailed information about intratumor, intertumoral and peritumor tissue.[8] The relationship of maximum standard glucose uptake with glucose transporter 1 (GLUT1) expression and the inverse correlation with glypican-3 (GPC3) expression was seen in patients with harboring liver tumors.[9] Additionally, Li et al found that the ^{18F}-FDG uptake of in hepatoma G2 (Hep G2) cells-expressed GPC3 significantly lower than that of RH7777 cells which has not expressed GPC3.[9] Moreover, ^{18F}-FDG uptake of the tumor to the non-tumor ratio of the EGF transgenic model of liver cancer was recorded to be dependent on lesion size and correlated with the upregulation of gene expression of glucose transporters and hexokinase isoenzymes.[10]

To develop effective treatments of liver tumors, the preclinical models are necessary to evaluate novel therapeutic agents and approach with consideration to their mechanism against liver tumors.[11] The *c-myc* transgenic mouse, a genetic model, developed a multiple highly malignant liver cancers promoted by *c-myc* oncogene mimic what happened in patients suffering from liver cancer.[12,13] The rationale of this study to investigatethe correlation of ^{18F}-FDG uptake and the gene expression related to glucose metabolism in different stages of liver cancer progression.

MATERIALS AND METHODS

Tumor Model and Animal Handling

All animal studies were approved by the Ethics Committee and the Local Governmental Authorities and were in accordance with national guidelines (Tier-Versuchs-Vorhaben 33.9-42502-04-08/1619). The *c-myc* transgenic mouse model is a well-identified model of hepatocellular carcinoma. Transgenic mice were generated by the method described by Dalemans et al.[14] In transgenic mice, the protooncogene *c-myc* is over-expressed under the promoter α1-antitrypsin, so that animals develop hepatocellular carcinoma at the age of about 12-months.

Altogether 96 transgenic (c-myc) and 48 non-transgenic CABL6 mice were examined. Mice were kept in cages with 1-4 mice per cage on sawdust on a 12-hours light-dark cycle, and 50% relative humidity, in a temperature-controlled (22 °C) room. Mice received a standard diet (Zucht, Specifications GmbH, DE, Germany, www.ssniff.de)[15] and drinking water *ad libitum*.

The 120 mice were divided into 6 groups, each group contained 12 mice of both sexes. DEN (Diethylnitrosamine) was injected intraperitoneally once a week during a period of 6-weeks while BHT was injected twice a week for 8-weeks at the age of 2-months, as explained earlier.[7]

In vivo microCT and microPET imaging were performed at four different time points (4, 5.5, 7 and 8.5-months) and all rats were sacrificed immediately after the end of imaging. All imaging procedures were carried out under inhalation anesthesia with isoflurane (Isoba vet., Essex Pharma, Germany) at a concentration of 4% for anesthesia induction and 1-2% for maintenance. Animals breathed spontaneously *via* nose cone (Summit Anesthesia Solutions, Bend, OR, USA). The breathing rate was continuously monitored using a small pressure transducer (Biovet, m2m imaging, Newark, NJ, USA) and kept between 80 and 100 per minute the mice were placed in a temperature-controlled bed for warming (T/Pump, Gaymar, Orchard Park, NY, USA). Recovery time was usually less than five-minutes after the imaging procedure.

MicroPET Imaging

All animals were starved for at least 6-hours before the imaging procedure. The anesthetized mice were injected intraperitoneally with 10 MBq of (18F)-2-Fluoro-2-deoxyglucose (^{18F}-FDG in a total volume of 50-100 µl sterile isotonic saline solution was obtained from the Department of Nuclear Medicine, Hannover Medical School, Hanover). After the injection, the CT scan was done and mice were kept in an anesthetic state and in the same position on the imaging bed until PET scan was carried out in order to minimize unspecific tracer enhancement in the muscles.[7,16,17]

Image Analysis

For microPET analysis, rigid registration of joint PET/CT datasets based on anatomical landmarks was used to generate fused datasets. Regions-of-interest (ROI) were manually detected in all focal liver and lung lesions with a diameter above and down 5 mm as detected in microCT and/or ^{18F}-FDG microPET. Exemplarily, FDG-uptake was estimated in 10 lesions below and up 5 mm as well. The background (non-tumor) signal was detected by placing an ROI in the tumor-free liver and lung parenchyma. The maximum count rate per volume was determined for each ROI and tumor-to-non-tumor ratios were calculated.[18]

Exon array expression: After animal imaging, all mice were sacrificed, the liver separated, weighted and [cryopreserved at-80 °C for ribonucleic acid (RNA) isolation later. The RNA extraction was carried out by using the RNeasy Micro Kit (Qiagen, Santa

Clarita, CA, USA). The extracted 47 RNA samples (3 males and 3 females per each 1st and 4th sacrifice of treated or non-treated groups) were tested for quality on the Agilent 2100 Bioanalyzer (Agilent Technologies, Palo Alto, USA). The RNA samples of RNA integrity number (RIN) above 2 were selected for exon array (Affymetrix). One mg of total RNA from individual animals of n=4 livers of treated or control transgenic either harbored tumor or normal control non-transgenic was used for Ribosomal RNA (rRNA) reduction and RNA labeling using the Invitrogen and Affymetrix kits, respectively, as we follow the manufacturer's instructions. Hybridization cocktails containing 4.5-5 mg of fragmented and end-labeled single-stranded sense target cDNA were previously prepared and hybridized to GeneChip Mouse Exon 1.0 ST arrays.[19,20] All processed arrays were scanned by using the GeneChip Scanner 3000 7G. Affymetrix Expression Console Software (version 1.0) was used to check the quality assessment and normalization NB. All steps of exon array experiment and analysis were done in Fraunhofer item for toxicology and experimental medicine, Hannover Germany 2010 and the analysis done in pharmacotoxico-genomics institute, MHH, Hannover Germany.

Statistical Analysis

Differential gene expression for exon array was analyzed by using two different software's, Array Track (v. 3.4.5) and Biotique X-RAY (v. 3.2). The following criteria were used for exon array differential gene expression study using the Biotique X-RAY software. One-way analysis of variance (ANOVA) was used for the glucose uptake difference between groups.

RESULTS

Transgenic ATT-MYC and non-transgenic mice at 2-months of age did not show any tumor growth or FDG uptake proved by CT and pet scans. Immediately after end the treatment, only one mouse out of 24 treated by diethylnitrosamine (DEN) had a gross tumor in the liver as confirmed by microCT and glucose uptake (pet scanning). The second, third and fourth sacrifices after the end of DEN treatment, all mice displayed liver tumor validated by histopathology (data not shown) and microCT and PET scanning.[7]

The ^{18F}-FDG uptake was ranged from 1 mm and up to 10 mm, strong or homogenous or weak in corresponding to the size of the tumor. The largest tumor size of above 10 mm was the highest glucose uptake. Also, glucose uptake was time-dependent as a fourth-time point of sacrifice >3rd>2nd>1st. Notably, the central tissue necrosis of the tumor was the weakest point of glucose uptake.

Interestingly, all non-transgenic or transgenic control groups didn't show any positive intensity for ^{18F}-FDG as well as non-genotoxic butylated hydroxytoluene (BHT).

The validation of PET *versus* CT accuracy revealed that pet scan is better tools for diagnosis of liver and lung cancer without any false positive echo that was seen in BHT treated mice and confirmed by previously by histopathological examination as big nodules encircle by lining endothelial cells.[7,16,17]

Additionally, primary lung cancer or liver cancer metastasis to lung, as reported in mice treated with DEN, has shown a correlation between glucose uptake and the tumor size as indicted by the strong signal intensity (Figures 1, 2 and 3).[7]

Figure 1. *^{18F}-FDG Uptake was Ranged from Low to High Intestacy in Liver Tissue Harbor Cancer Cells in c-myc Treated by DEN at Age of 8.5-Months*

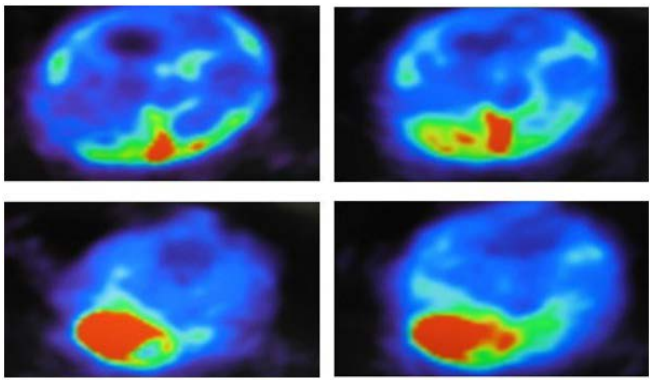

Figure 2. *The Depicted Figure Shown The Evidence of Glucose Uptake in Primary Lung Cancer Tissue and Also Correlated with Size Dependent in c-myc Treated by DEN at Age of 8.5-months or After 4.5-Monthes After End of Treatment*

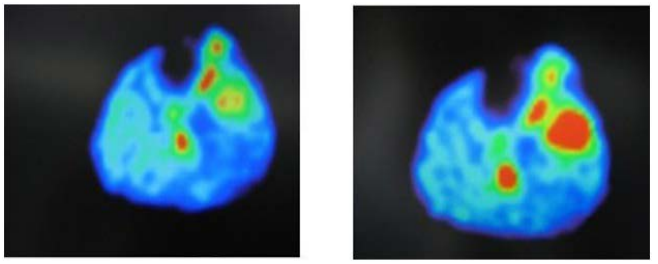

Figure 3. *The Depicted Figure Shown the Highest Glucose Uptake (means±se) in Liver Harbor HCC in the Last Sacrifice after DEN Treatment at Age of 8.5-months (B). Notably, DEN Treated Transgenic Mice of Both First (A) and Last Sacrifice (B) Displayed a Significant Increase of Glucose Uptake when Compared with Transgenic Mice Treated by BHT or Corn Oil as Vehicle Groups*

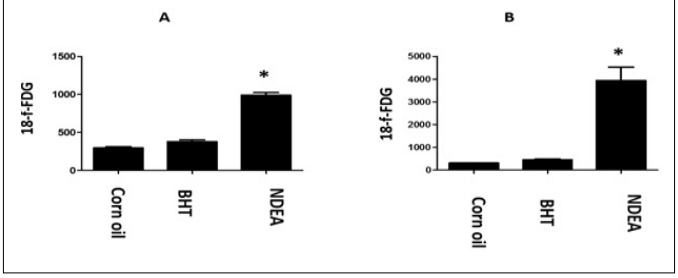

Gene Expression Related to Glucose Metabolism Analyzed by Biotiqe System

We studied 12 hybridizations comparison of 1st sacrifice of DEN genotoxic carcinogens *versus* non-genotoxic one were analyzed by the biotique system, it was found that among the top 10-fold changes in genes with significant differential gene expression was *Slc38a2* and no ultra-splicing in *glut1* or *2*. Fold change is in terms of the normalized untransformed data.

In the present, we study the biotiqe analysis of 9 hybridizations of the Mouse Exon 10-ST array using mixed model analysis of variance. We found that there is no genes or alternative splicing between top 10 significant genes expressed in the groups *DEN_1* sacrifice *_mf* when compared to *ntr_4s_mf* related to glucose metabolism (Table 1).

Here in Table 2, the genes responsible of glucose transport such as of *glut1, 3, 4*, *hk1*, *slc1a5*, *slc5a1*, *slc1a4*, *slc1a2*, *gp6c* and *gpc-1-3-4* were shown a significant regulation at *p*-value≤0.05 while *glut2* (fold change 0.9503, *p*-value 0.4385) and *hk2* (fold change 3.0589, *p*-value 0.0565) were shown a non-significant in-

Table 1. *Shows the slc38a2 gene Expression Related to Glucose Metabol as with Significant Differential Gene Expression in Liver Tissue of 1st Sacrifice After DEN when Compared with BHT and Related to Glucose Metabolism. Fold Change was in Terms of the Normalized Untransformed Data*

Gene Symbol	T Cluster ID	Description	Fold Change	Differential Expression *p* value
Slc38a2	6838257	solute carrier family 38 member 2 (among its pathway glucose transport)	2.31	0.02

Table 2. *The Gene Expression of glut1, 3, 4, hk1, slc1a5, slc5a1, slc1a4, slc1a2, gp6c and gpc-1-3-4 at p-value≤0.05 while glut2 and hk2 were Shown a Non-significant Expression Immediately after DEN Treatment at 4-months Aged Mice when Compared to BHT Treatment and Control Group*

Gene Symbol	T Cluster ID	Description	Fold Change	*p* value
Hk1	15275	Hexokinase-1	4.0457	0.0243
Slc1a5	20514	Solute carrier family 1 member 5	12.8096	0.0001
Slc5a1	20537	Solute carrier family 5 (sodium/glucose cotransporter), member 1	5.7203	0.0068
Slc1a4	55963	Solute carrier family 1 (glutamate/neutral amino acid transporter), member 4	3.2237	0.0488
Slc1a2	20511	Solute carrier family 1 (glial high affinity glutamate transporter), member 2	4.442	0.0177
Slc38a2	67760	Solute carrier family 38 member 2 (among its pathway glucose transport)	17.2678	0
Slc2a1	20525	Glut1	11.2042	0.0003
Slc2a2	2056	Glut2	0.9503	0.4385
Slc2a3	20527	Glut3	10.5845	0.0004
Slc2a4	20528	Glut4	4.5084	0.0168
HK2	15277	Hexokinase-2	3.0589	0.0565
Gpc1	14733	Glypican-1	25.5662	0
Gpc3	14734	Glypican-3	5.6451	0.0072
Gpc4	14735	Glypican-4	5.5982	0.0074
G6pc	14377	Glucose 6 phosphatase	4.823	0.0131
ALDOA	11674	Aldolase A	9.6925	0.0006
PKM2	18746	Pyruvate kinase M2v	2.3168	0.0668
LDHB	16832	Lactate dehydrogenase wasoform	2.874	0.4593
Six1	427402	SIX Homeobox 1	0.7143	0.0191
HIF1a	432128	Hypoxemia inducing factor 1a	4.343	0.0001
c-myc	424405	Myelocytomatoswas	14.0755	0.5274
Pfkl	427329	Phosphofructokinase	0.7684	--
Pgk1	427956	Phosphoglycerate kinase-1	Not found	--
Pgam1	424483	Phosphoglycerate Mutase 1	Not found	0.0003
Trp53	424011	Tumor suppressor p53	10.8355	2.60

Table 3. *The Gene Expression of slc1a5, slc38a2, glut1, glut4 and gpc-3,4 Genes were Expressed Significantly with Fold Changes in Liver Tissue of DEN Treated Mice at the Age of 8.5 when Compared to BHT or Control Transgenic or Non-transgenic One. While hk, 2, slc5a1, slc1a4, glut2, gut3, g6pc and gpc-1 were Expressed in a Non-significant State when Compared to BHT or Control Transgenic or Non-transgenic One*

Gene Symbol	T Cluster ID	Description	Fold Change	*Differential Expression p* value
Hk1	15275	Hexokinase-1	0.8593	0.2513
Slc1a5	20514	Solute carrier family 1 member 5	0.4737	0.0046
Slc5a1	20537	Solute carrier family 5 (sodium/glucose cotransporter), member 1	2.0376	0.14672
Slc1a4	55963	Solute carrier family 1 (glutamate/neutral amino acid transporter), member 4	0.64070	0.5992
Slc1a2	20511	Solute carrier family 1 (glial high affinity glutamate transporter), member 2	2.5437	0.0905
Slc38a2	67760	Solute carrier family 38 member 2 (among its pathway glucose transport)	3.2134	0.0493
Slc2a1	20525	Glut1	3.849	0.0286
Slc2a2	20526	Glut2	3.0446	0.0572
Slc2a3	20527	Glut3	2.0203	0.1493
Slc2a4	20528	Glut4	3.4199	0.0411
HK2	15277	Hexokinase-2	2.1573	0.1307
Gpc1	14733	Glypican-1	2.3751	0.1061
Gpc3	14734	Glypican-3	6.4366	0.0041
Gpc4	14735	Glypican-4	2.5828	0.0873
G6pc	14377	Glucose 6 phosphatase	2.9161	0.0643
ALDOA	11674	Aldolase A	4.0709	0.0238
PKM2	18746	Pyruvate kinase M2v	1.5475	0.2387
LDHB	16832	Lactate dehydrogenase wasoform	2.7194	0.0769
Six1	427402	SIX Homeobox 1	0.488	0.6951
HIF1a	432128	Hypoxemia inducing factor 1a	0.7197	0.5539
c-myc	424405	Myelocytomatoswas	8.3895	0.0012
Pfkl	427329	Phosphofructokinase	6.0835	0.0053
Pgk1	427956	Phosphoglycerate kinase-1	Not found	--
Pgam1	424483	Phosphoglycerate Mutase 1	Not found	--
Trp53	424011	Tumor suppressor p53	5.9049	0.0059

crease at age of 4-months or at the end of treatment.

Notably, in Table 3, the genes responsible of glucose transport of *slc1a5*, *slc38a2*, *glut1, glut4* and *gpc-3,4* displayed significant fold changes in tumor tissue of DEN treated mice when compared to BHT or control transgenic or non-transgenic one. While *hk1, 2*, *slc5a1*, *slc1a4*, *glut2, glut3, g6pc* and *gpc-1* genes were shown a non-significant increase when compared to the control group.

Regarding the glycolytic gene *pathways*, *c-myc*, *hif-1a and aldolase-a (aldoa)* were expressed both at time point of 4 and 8.5 months while lactate dehydrogenase, hexokinase-2 and pyruvate kinase M2 (PKM2) increased non significantly in DEN treatment when compared to BHT or control non-transgenic animals see Tables 3 and 4.

DISCUSSION

The use of these animal models help to study the biology of the human tumor as well as the technology of geneexpression for discovering the genes that helpful for developing or testing anticancer therapeutic agents before the different stages of clinical evaluation safety.

It was previously reported by us[7,16,17] that MicroCT, PET or joined MicoCT/PET for identification of acceleration liver tumor in ATT-MYC transgenic mouse model of liver cancer induced by DEN and validation of these finding by histopathological examination. While BHT fails to promote liver cancer in transgenic[7,16,17] and in non-transgenic mice.[21,22]

False-positive echo was recorded by us in BHT treatment by MicroCT, while histopathological finding proof that BHT fails to promote liver tumor until 8.5-months and only induced large dysplastic nodules lined by endothelial cells.[7] Notably, pet imaging was a goodtool as BHT treated transgenic mice had no evidence of glucose uptake until 8.5-months as well as control groups and also validated by histopathlogical examination previously. In contrast, the uptake of FDG could increase and in nor-

Table 4. *Shows the Microarray Analyses of the Whole Liver Genome of att-myc at 12-months Without Treatment of Up-regulation of hk1,slc1a5, slc5a1,slc1a4, slc1a2 and gpc1,3. While glut1, 2,3,4, slc38a2, gpc4, g6pc and hk2 were Reported Non-significant when Compared to BHT Treatment and Non-transgenic Mice*

Gene Symbol	T Cluster ID	Description	Fold Change	*Differential Expression p* value
Hk1	15275	Hexokinas1	2.06880	0.022
Slc1a5	20514	Solute carrier family 1 number 5	8.498	0.0009
Slc5a1	20537	Solute carrier family 5 (sodium/glucose cotransporter), member 1	4.8465	0.015
Slc1a4	55963	Solute carrier family 1 (glutamate/neutral amino acid transporter), member 4	2.9	0.0009
Slc1a2	20511	Solute carrier family 1 (glial high affinity glutamate transporter), member 2	2.68	0.0001
Slc38a2	67760	Solute carrier family 38 member 2 (among its pathway glucose transport)	1.1012	0.5983
Slc2a1	20525	Glut1	2.0599	0.1129
Slc2a2 Glut2	20526	Glut2	1.0098	0.9558
Slc2a3	20527	Glut3	1.7805	0.1104
Slc2a4	20528	Glut4	0.338	1.5796
HK2	15277	Hexokinase2	3.1893	0.1963
Gpc1	14733	Glypican-1	0.0425	0.0425
Gpc3	14734	Glypican-3	3.8882	0.0425
Gpc4	14735	Glypican-4	1.0373	0.7924
G6pc	14377	Glucose 6 phosphatase	1.8741	0.0745
ALDOA	11674	Aldolase A	1.9602	0.0001
PKM2	18746	Pyruvate kinase M2v	0.0754	1.6485
LDHB	16832	Lactate dehydrogenase isoform	2.3694	0.0618
Six1	427402	SIX Homeobox 1	2.1361	0.1221
HIF1a	432128	Hypoxemia inducing factor 1a	1.6606	0.0041
c-myc	424405	Myelocytomatoswas	32.049	0
Pfkl	427329	Phosphofructokinase	1.4353	0.0163
Pgk1	427956	Phosphoglycerate kinase-1	1.2137	0.0144
Pgam1	424483	Phosphoglycerate Mutase 1	1.2437	0.0341
Trp53	424011	Tumor suppressor p53	4.786	0.0002

mal tissue, some tumors did not show FDG uptake.[23]

Interestingly, PET/CT imagining enables non-invasive information about tumor size, non-tumor tissue, metastasis, multiple tissue tumors[7] and detected of the presence of tissue necrosis by hyper-intensity and hypo-intensity of FDG uptake.[24] Also, DEN enhanced liver tumor growth and FDG uptake in a time-dependent manner after the end of treatment.[7]

The gene expression in liver cancer and glucose uptake detected by PET imaging consider a new tools for study liver tumor.[8] In the current study, GPC-3 was expressed in ATT-MYC mice at one year and at different time points after DEN treatment and correlated positively with the presence and size of the liver tumor as well as GPC3 expression was observed in 67.3% of HCC patients and 75.0% of them characterized by moderately differentiated HCC and the other with poorly differentiated HCC.[9]

Glut1 and *hexokinase 1* were regulated in ATT-MYC mice at one-year and at a time point after DEN treatment and correlated positively with the presence and size of the liver tumor as a similar result seen in epidermal growth factor (EGF) hepatocellular carcinoma in a transgenic model of liver cancer[10] or human liver cancer or in Hep G2.[9] Also, there was a link between ^{18F}-FDG high uptake and the expression levels of the glycolytic pathway genes as *GLUT1, hexokinase 1, 2, 3* in Primary macronodular adrenal hyperplasia.[25] In contrast, *GLUT1* expression does not correlate significantly with ^{18F}-FDG uptake in colorectal carcinoma,[26-28] neuroendocrine tumor,[29] in thymic epithelial tumors[30] and pancreatic tumor.[31]

Up withstanding to our result, the ^{18F}-FDG uptake was increased in primary lung cancer promoted by DEN and *c-myc* promotion[32] or HCC secondary metastases to lung tissue. Similarly, ^{18F}-FDG uptake occurrence of colorectal hepatic tissue after hepatectomy.[33] The cancer cells had characteristic features in their own metabolic process, such as the increasing uptake of glucose by tumor cells enhanced metabolic shifts to uncontrolled cell growth and survival.[34] Also, the expression of *aldoa* gene as a glycolytic pathway in both liver tumors in ATT-MYC micetreated with or without DEN treatment was as a common feature of oc-

currence HCC.[35] Notably, the overexpression of transcriptional factors, c-myc hypoxia-inducible factor and glycolytic enzymes were accompanied by poor prognosis and may be associated with resistance or failure of chemoradiotherapy in multiple gastrointestinal cancer cell types.[36] So, the significance of the clinical impact of the Warburg effect in tumor growth reflects the important roles of inhibition of glycolytic pathway as significant biomarkers for predicting cancer prognosis and antitumor drug therapy[37] especially with small interfering RNA (siRNA) as miR-338/PFKL.

CONCLUSION

There is a definitive correlation between genes responsible for glucose transport, ^{18F}-FDG uptake in the early and advanced stages of liver cancer progressions such as *glut1*, *HK1*, GPC3 and other alternative pathways of glucose metabolism. This finding reveal the important roles of inhibition of the glycolytic pathway as antitumor drug therapy.

ACKNOWLEDGMENT

We thank Roman Haltera postdoctoral researcher who helped during the experimental part done in Fraunhofer Institute of Toxicology and Experimental Medicine (Hanover, Germany). Also, we thank Keritina Wiesner technician, who shared and helped in most of the exon-array experiment. Moreover, we had grateful to Tatiana Miere, a postdoctoral researcher, who supported us in learning gene expression on array track, X-RAY (version 3.2) software and the Excel add-in from Biotique Systems Inc (Reno, NV, USA).

CONFLICTS OF INTEREST

The authors declare that they have no conflicts of interest.

REFERENCES

1. Pinheiro PS, Callahan KE, Jones PD, Morris C, Ransdell JM, Kwon D, et al. Liver cancer: A leading cause of cancer death in the United States and the role of the 1945-1965 birth cohort by ethnicity. *JHEP Rep.* 2019; 1(3): 162-169. doi: 10.1016/j.jhepr.2019.05.008

2. Choo SP, Tan WL, Goh BK, Tai WM, Zhu AX. Comparison of hepatocellular carcinoma in Eastern versus Western populations. *Cancer.* 2016; 122(22): 3430-3446. doi: 10.1002/cncr.30237

3. Bray F, Ferlay J, Soerjomataram I, Siegel RL, Torre LA, Jemal A. Global cancer statistics 2018: GLOBOCAN estimates of incidence and mortality worldwide for 36 cancers in 185 countries. *CA Cancer J Clin.* 2018; 68(6): 394-424. doi: 10.3322/caac.21492

4. Rawla P, Sunkara T, Muralidharan P, Raj JP. Update in global trends and aetiology of hepatocellular carcinoma. *Contemp Oncol (Pozn).* 2018; 22(3): 141-150. doi: 10.5114/wo.2018.78941

5. Omar A, Abou-Alfa GK, Khairy A, Omar H. Risk factors for developing hepatocellular carcinoma in Egypt. *Chin Clin Oncol.* 2013; 2(4): 43. doi: 10.3978/j.issn.2304-3865.2013.11.07

6. Dimitroulis D, Damaskos C, Valsami S, Davakis S, Garmpis N, Spartalis E, et al. From diagnosis to treatment of hepatocellular carcinoma: An epidemic problem for both developed and developing world. *World J Gastroenterol.* 2017; 23(29): 5282-5294. doi: 10.3748/wjg.v23.i29.5282

7. Hueper K, Elalfy M, Laenger F, Halter R, Rodt T, Galanski M, et al. PET/CT imaging of c-Myc transgenic mice identifies the genotoxic N-nitroso-diethylamine as carcinogen in a short-term cancer bioassay. *PLoS One.* 2012; 7(2): e30432. doi: 10.1371/journal.pone.0030432

8. Bai HX, Lee AM, Yang L, Zhang P, Davatzikos C, Maris JM, et al. Imaging genomics in cancer research: Limitations and promises. *Br J Radiol.* 2016; 89(1061): 20151030. doi: 10.1259/bjr.20151030

9. Li Y-C, Yang C-S, Zhou W-L, Li H-S, Han Y-J, Wang Q-S, et al. Low glucose metabolism in hepatocellular carcinoma with GPC3 expression. *World J Gastroenterol.* 2018; 24(4): 494-503. doi: 10.3748/wjg.v24.i4.494

10. von Falck C, Rodt T, Halter R, Spanel R, Galanski M, Borlak J. Combined microPET/CT for imaging of hepatocellular carcinoma in mice. *Front Biosci (Landmark Ed).* 2009; 14: 2193-2202. doi: 10.2741/3371

11. Bibby M. Orthotopic models of cancer for preclinical drug evaluation: Advantages and disadvantages. *Eur J Cancer.* 2004; 40(6): 852-857. doi: 10.1016/j.ejca.2003.11.021

12. Calvisi DF, Thorgeirsson SS. Molecular mechanisms of hepatocarcinogenesis in transgenic mouse models of liver cancer. *Toxicol Pathol.* 2005; 33(1): 181-184. doi: 10.1080/01926230590522095

13. Soucek L, Whitfield J, Martins CP, Finch AJ, Murphy DJ, Sodir NM, et al. Modelling Myc inhibition as a cancer therapy. *Nature.* 2008; 455(7213): 679-683. doi: 10.1038/nature07260

14. Dalemans W, Perraud F, Le Meur M, Gerlinger P, Courthey M, Pavirani A. Heterologous protein expression by transimmortalized differentiated liver cell lines derived from transgenic mice (hepatomas/α1 antitrypsin/ONC mouse). *Biologicals.* 1990; 18(3): 191-198. doi: 10.1016/1045-1056(90)90006-l

15. Ssniff Spezialdiaten. ssniff Web site. http://www.ssniff.de/. Accessed January 16, 2020.

16. Hueper K, Elalfy M, Länger F, Halter R, Rodt T, Vaske B, et al. MikroCT und mikroPET zur beurteilung und quantifizierung der leberzellkarzinom-entstehung im rahmen einer toxikologischen untersuchung im transgenen mausmodell [In: German]. *RöFo - Fortschritte auf dem Gebiet der R.* 2010; 182(11). doi: 10.1055/s-0030-1268295

17. Hueper K, Elalfy M, Länger F, Halter R, Rodt T, Hartung

D, et al., editors. Einsatz der in vivo µCT und 18F-FDG-µPET Bildgebung zur frühzeitigen Identifizierung von Karzinogenen in einem transgenen Mausmodell der Leberzellkarzinomentstehung. *RöFo - Fortschritte auf dem Gebiet der R.* 2011; 183(S 01): doi: 10.1055/s-0031-1279558

18. Weber SM, Peterson KA, Durkee B, Qi C, Longino M, Warner T, et al. Imaging of murine liver tumor using microCT with a hepatocyte-selective contrast agent: Accuracy is dependent on adequate contrast enhancement. *J Surg Res.* 2004; 119(1): 41-45. doi: 10.1016/S0022-4804(03)00357-3

19. Londhe KB, Borlak J. A cross-platform comparison of genome-wide expression changes of laser microdissected lung tissue of C-Raf transgenic mice using 3' IVT and exon array. *PLoS One.* 2012; 7(7): e40778. doi: 10.1371/journal.pone.0040778

20. Liu Y-C, Li F, Handler J, Huang CRL, Xiang Y, Neretti N, et al. Global regulation of nucleotide biosynthetic genes by c-Myc. *PLoS One.* 2008;3(7): e2722. doi: 10.1371/journal.pone.0002722

21. Lee J-S, Chu I-S, Mikaelyan A, Calvisi DF, Heo J, Reddy JK, et al. Application of comparative functional genomics to identify best-fit mouse models to study human cancer. *Nat Genet.* 2004; 36(12): 1306-1311. doi: 10.1038/ng1481

22. Mahmoud EM. Limitation of Liver tumor promoting properties of butylated hydroxytoluene in non-transgenic C57BL6 black mouse. 2016; 6(1): 1-6.

23. Long NM, Smith CS. Causes and imaging features of false positives and false negatives on 18 F-PET/CT in oncologic imaging. *Insights Imaging.* 2011; 2(6): 679-698. doi: 10.1007/s13244-010-0062-3

24. Zhao J, Zhang Z, Nie D, Ma H, Yuan G, Su S, et al. PET Imaging of Hepatocellular Carcinomas: 18F-Fluoropropionic Acid as a Complementary Radiotracer for 18F-Fluorodeoxyglucose. *Mol Imaging.* 2019; 18: 1536012118821032. doi: 10.1177/1536012118821032

25. Cavalcante IP, Zerbini MCN, Alencar GA, Mariani BdP, Buchpiguel CA, Almeida MQ, et al. High 18F-FDG uptake in PMAH correlated with normal expression of Glut1, HK1, HK2, and HK3. *Acta Radiol.* 2016; 57(3): 370-377. doi: 10.1177/0284185115575195

26. Hong R, Lim S-C. 18F-fluoro-2-deoxyglucose uptake on PET CT and glucose transporter 1 expression in colorectal adenocarcinoma. *World J Gastroenterol.* 2012; 18(2): 168-174. doi: 10.3748/wjg.v18.i2.168

27. Xu H-L, Li M, Zhang R-J, Jiang H-J, Zhang M-Y, Li X, et al. Prediction of tumor biological characteristics in different colorectal cancer liver metastasis animal models using 18F-FDG and 18F-FLT. *Hepatobiliary Pancreat Dis Int.* 2018; 17(2): 140-148. doi: 10.1016/j.hbpd.2018.03.006

28. Rahmim A, Bak-Fredslund KP, Ashrafinia S, Lu L, Schmidtlein CR, Subramaniam RM, et al. Prognostic modeling for patients with colorectal liver metastases incorporating FDG PET radiomic features. *Eur J Radiol.* 2019; 113: 101-109. doi: 10.1016/j.ejrad.2019.02.006

29. Kaira K, Murakami H, Endo M, Ohde Y, Naito T, Kondo H, et al. Biological correlation of 18F-FDG uptake on PET in pulmonary neuroendocrine tumors. *Anticancer Res.* 2013; 33(10): 4219-4228.

30. Kaira K, Endo M, Abe M, Nakagawa K, Ohde Y, Okumura T, et al. Biologic correlation of 2-[18F]-fluoro-2-deoxy-D-glucose uptake on positron emission tomography in thymic epithelial tumors. *J Clinical Oncol.* 2010; 28(23): 3746-3753. doi: 10.1200/JCO.2009.27.4662

31. Kaida H, Azuma K, Kawahara A, Yasunaga M, Kitasato Y, Hattori S, et al. The correlation between FDG uptake and biological molecular markers in pancreatic cancer patients. *Eur J Radiol.* 2016; 85(10): 1804-1810. doi: 10.1016/j.ejrad.2016.08.007

32. Bolton RCD, Calapaquí-Terán AK, Giammarile F, Rubello D. Role of 18F-FDG-PET/CT in establishing new clinical and therapeutic modalities in lung cancer. *Rev Esp Med Nucl Imagen Mol.* 2019; 38(4): 229-233. doi: 10.1016/j.remn.2019.02.003

33. Shim J-R, Lee SD, Han S-S, Lee SJ, Lee DE, Kim S-K, et al. Prognostic significance of 18F-FDG PET/CT in patients with colorectal cancer liver metastases after hepatectomy. *Eur J Surg Oncol.* 2018; 44(5): 670-676. doi: 10.1016/j.ejso.2018.01.243

34. Fadaka A, Ajiboye B, Ojo O, Adewale O, Olayide I, Emuowhochere R. Biology of glucose metabolization in cancer cells. *J Oncol Sci.* 2017; 3(2): 45-51. doi: 10.1016/j.jons.2017.06.002

35. Lee NC, Carella MA, Papa S, Bubici C. High expression of glycolytic genes in cirrhosis correlates with the risk of developing liver cancer. *Front Cell Dev Biol.* 2018; 6: 138. doi: 10.3389/fcell.2018.00138

36. Sawayama H, Ishimoto T, Sugihara H, Miyanari N, Miyamoto Y, Baba Y, et al. Clinical impact of the Warburg effect in gastrointestinal cancer. *Int J Oncol.* 2014; 45(4): 1345-1354. doi: 10.3892/ijo.2014.2563

37. Zheng J, Luo J, Zeng H, Guo L, Shao G. 125I suppressed the Warburg effect viaregulating miR-338/PFKL axis in hepatocellular carcinoma. *Biomed Pharmacother.* 2019; 119: 109402. doi: 10.1016/j.biopha.2019.109402